

THIS IS ONLY A DRAFT

This is only a draft: appendix are empty for now. Code will be either attached here in the pdf or in the drive folder.

Abstract

Aircraft dynamics is dominated by parameters uncertainties. The more common way to deal with uncertainties is gain scheduling that is time consuming. Many robust and adaptive techniques have been applied in the past, but only recently the computing power and theoretical knowledge in terms of stability are mature to apply those technique to real world application.

L1 Adaptive control is one of the latest advancement in the field of adaptive control systems, and guarantees that in presence of uncertainties the system remains stable.

In this project a fixed-wing aircraft is simulated and a baseline controller is designed following the pole-placement methods. L1AC tries to compensate for the uncertainties within the control bandwidth of the actuator.

Parameters uncertainties is added on purpose to test the robustness of the control scheme.

Chapter 1

Aircraft Model

This chapter describes the aircraft equations employed for the simulation of the system dynamics.

1.1 Aerodynamic Forces

The aerodynamic forces are modeled by aerodynamic coefficients. These are modeled as follows:

$$L = \frac{1}{2}\rho V^2 S C_L \quad (1.1a)$$

$$D = \frac{1}{2}\rho V^2 S C_D \quad (1.1b)$$

$$Y = \frac{1}{2}\rho V^2 S C_Y \quad (1.1c)$$

The coefficients are modeled in the following way:

$$C_L = C_{L0} + C_{L\alpha}\alpha + C_{Leq}\frac{c}{2V} q + C_{L\delta e}\delta e \quad (1.2a)$$

$$C_D = C_{D0} + \frac{C_L^2}{\pi e A R} \quad (1.2b)$$

$$C_Y = C_{Y\beta}\beta + C_{Y\delta r}\delta r \quad (1.2c)$$

1.2 Aerodynamic Moments

The aerodynamic moments acting on the fixed-wing aircraft are:

$$l = \frac{1}{2} \rho V^2 S b C_l \quad (1.3a)$$

$$M = \frac{1}{2} \rho V^2 S c C_m \quad (1.3b)$$

$$N = \frac{1}{2} \rho V^2 S b C_n \quad (1.3c)$$

The coefficients are modeled in the following way:

$$C_l = C_{l\beta}\beta + C_{lp}\frac{b}{2V}p + C_{lr}\frac{b}{2V}r + C_{l\delta a}\delta a + C_{l\delta r}\delta r \quad (1.4a)$$

$$C_m = C_{m0} + C_{m\alpha}\alpha + C_{meq}\frac{c}{2V}q + C_{m\delta e}\delta e \quad (1.4b)$$

$$C_n = C_{n\beta}\beta + C_{np}\frac{b}{2V}p + C_{nr}\frac{b}{2V}r + C_{n\delta a}\delta a + C_{n\delta r}\delta r \quad (1.4c)$$

1.3 Engine Model

The thrust has been modeled parallel to the x-body axis, hence $Y_T = Z_T = 0$ and there is no pitch moment contribution:

$$X_T = T_{delivered} = \delta t \cdot T_{max} \quad (1.5)$$

1.4 Model Equations

To derive a complete description in differential equations form, nonlinear equations that can be founded in [?] are provided. The translation accelerations are described by the well known equations:

$$\mathbf{F} = m \left(\frac{\partial \mathbf{V}}{\partial t} + \boldsymbol{\Omega} \times \mathbf{V} \right) \quad (1.6a)$$

$$\mathbf{F} = [\Sigma \mathbf{X}, \Sigma \mathbf{Y}, \Sigma \mathbf{Z}]^T \quad (1.6b)$$

$$\mathbf{V} = [u, v, w]^T \quad (1.6c)$$

$$\boldsymbol{\Omega} = [p, q, r]^T \quad (1.6d)$$

$$\frac{\partial \mathbf{V}}{\partial t} = \frac{1}{m} \mathbf{F} - \boldsymbol{\Omega} \times \mathbf{V} \quad (1.6e)$$

Where the \mathbf{F} is the vector of the total forces in body axis, \mathbf{V} is the velocity vector in body axis and $\boldsymbol{\Omega}$ is the rotational velocity in body reference frame.

For the rotational acceleration:

$$\mathbf{M} = \frac{\partial \mathbf{I}\boldsymbol{\Omega}}{\partial t} + \boldsymbol{\Omega} \times \mathbf{I}\boldsymbol{\Omega} \quad (1.7a)$$

$$\mathbf{I} \frac{\partial \boldsymbol{\Omega}}{\partial t} = \mathbf{M} - \boldsymbol{\Omega} \times \mathbf{I}\boldsymbol{\Omega} \quad (1.7b)$$

$$\dot{\boldsymbol{\Omega}} = \frac{\partial \boldsymbol{\Omega}}{\partial t} \quad (1.7c)$$

Where \mathbf{M} is the vector of the moment in body axis \mathbf{I} is the inertia matrix and $\dot{\boldsymbol{\Omega}}$ is the angular rotation acceleration.

The transformation from wind-axis to body-axis is defined:

$$u = V \cos \alpha \cos \beta \quad (1.8a)$$

$$v = V \sin \beta \quad (1.8b)$$

$$w = V \sin \alpha \cos \beta \quad (1.8c)$$

and for the inverse transformation:

$$V = |V| = \sqrt{(u^2 + v^2 + w^2)} \quad (1.9a)$$

$$\alpha = \tan^{-1} \left(\frac{w}{V} \right) \quad (1.9b)$$

$$\beta = \sin^{-1} \left(\frac{v}{V} \right) \quad (1.9c)$$

The complete set of equations used for simulation are reported:

$$\begin{aligned} \dot{V} &= \frac{1}{m} [-D \cos \beta + Y \sin \beta + X_T \cos \alpha \cos \beta + Y_T \sin \beta + Z_T \sin \alpha \cos \beta \\ &\quad - mg (\cos \alpha \cos \beta \sin \theta - \sin \beta \sin \phi \cos \theta - \sin \alpha \cos \beta \cos \phi \cos \theta)] \end{aligned} \quad (1.10)$$

$$\begin{aligned} \dot{\alpha} &= \frac{1}{Vm \cos \beta} [-L + Z_T \cos \alpha - X_T \sin \alpha + mg (\cos \alpha \cos \phi \cos \theta + \sin \alpha \sin \theta)] \\ &\quad + q - \tan \beta (p \cos \alpha + r \sin \alpha) \end{aligned} \quad (1.11)$$

$$\begin{aligned}\dot{\beta} = \frac{1}{V_m} & [D \sin \beta + Y \cos \beta - X_T \cos \alpha \sin \beta + Y_T \cos \beta - Z_T \sin \alpha \sin \beta \\ & + mg (\cos \alpha \sin \beta \sin \theta + \cos \beta \sin \phi \cos \theta - \sin \alpha \sin \beta \cos \phi \cos \theta)] \\ & + p \sin \alpha - r \cos \alpha\end{aligned}\quad (1.12)$$

Where D is the aerodynamic drag, Y is the lateral side force, L is the aerodynamic lift. Then X_T , Y_T , Z_T are the propulsive forces in body axis.

The equations regarding $\dot{\Omega}$ that are part of the state are more precisely, with the assumption that the matrix of inertia \mathbf{I} is diagonal, the following:

$$\dot{p} = \frac{l + (I_y - I_z) qr}{I_x} \quad (1.13a)$$

$$\dot{q} = \frac{M + (I_x - I_z) pr}{I_y} \quad (1.13b)$$

$$\dot{r} = \frac{N + (I_x - I_y) pq}{I_z} \quad (1.13c)$$

The equations for the attitude in Euler's angles are reported:

$$\dot{\Omega} = \mathbf{R} \frac{\partial \mathbf{E}}{\partial t} \quad (1.14a)$$

Where \mathbf{E} is the attitude vector of the Euler's angle, and \mathbf{R} the matrix that transform angular velocities in earth-fixed axis system into body axis angular velocities.

$$\mathbf{E} = [\phi, \theta, \psi]^T \quad (1.15a)$$

$$\mathbf{R} = \begin{bmatrix} 1 & 0 & -\sin \theta \\ 0 & \cos \phi & \sin \phi \cos \theta \\ 0 & -\sin \phi & \cos \phi \cos \theta \end{bmatrix} \quad (1.16)$$

Therefore:

$$\frac{\partial \mathbf{E}}{\partial t} = \mathbf{R}^{-1} \dot{\Omega} \quad (1.17a)$$

That expanded are:

$$\dot{\phi} = p + q \sin \phi \tan \theta + r \cos \phi \tan \theta \quad (1.18a)$$

$$\dot{\theta} = q \cos \phi - r \sin \phi \quad (1.18b)$$

$$\dot{\psi} = q \sin \phi \sec \theta + r \cos \phi \sec \theta \quad (1.18c)$$

The L_{BE} that transforms vector from earth axis system into the body axis system is:

$$\begin{aligned} L_{BE} &= \begin{bmatrix} \cos \psi & -\sin \psi & 0 \\ \sin \psi & \cos \psi & 0 \\ 0 & 0 & 1 \end{bmatrix} \begin{bmatrix} \cos \theta & 0 & \sin \theta \\ 0 & 1 & 0 \\ -\sin \theta & 0 & \cos \theta \end{bmatrix} \begin{bmatrix} 1 & 0 & 0 \\ 0 & \cos \phi & -\sin \phi \\ 0 & \sin \phi & \cos \phi \end{bmatrix} = \\ &= \begin{bmatrix} \cos \theta \cos \psi & \cos \theta \sin \psi & -\sin \theta \\ \sin \phi \sin \theta \cos \psi - \cos \phi \sin \psi & \sin \phi \sin \theta \sin \psi + \cos \phi \cos \psi & \sin \phi \cos \theta \\ \cos \phi \sin \theta \cos \psi + \sin \phi \sin \psi & \cos \phi \sin \theta \sin \psi - \sin \phi \cos \psi & \cos \phi \cos \theta \end{bmatrix} \quad (1.19) \end{aligned}$$

The velocities in Earth-fixed coordinate \mathbf{V}_E are related to the corresponding Body axis velocities \mathbf{V}_B by:

$$\mathbf{V}_B = L_{BE} \mathbf{V}_E \quad (1.20)$$

where

$$\mathbf{V}_B = [u, v, w]^T \quad (1.21)$$

and

$$\mathbf{V}_E = [V_N, V_E, V_D]^T \quad (1.22)$$

A formulation describing the earth velocities V_E starting from the body ones V_B , can hence been derived:

$$\mathbf{V}_E = L_{BE}^{-1} \mathbf{V}_B \quad (1.23)$$

In an expanded way noting that the position in earth axis $\mathbf{P}_E = [x_N, y_E, z_D]^T$ and that $\dot{\mathbf{P}}_E = \mathbf{V}_E$:

$$\dot{h} = V (\cos \alpha \cos \beta \sin \theta - \sin \beta \sin \phi \cos \theta - \sin \alpha \cos \beta \cos \phi \cos \theta) \quad (1.24)$$

$$\begin{aligned} \dot{x}_N &= V [\cos \alpha \cos \beta \cos \theta \cos \psi + \sin \beta (\sin \phi \sin \theta \cos \psi - \cos \phi \sin \psi) \\ &\quad + \sin \alpha \cos \beta (\cos \phi \sin \theta \cos \psi + \sin \phi \sin \psi)] \quad (1.25) \end{aligned}$$

$$\begin{aligned} \dot{y}_E &= V [\cos \alpha \cos \beta \cos \theta \sin \psi + \sin \beta (\cos \phi \cos \psi + \sin \phi \sin \theta \sin \psi) \\ &\quad + \sin \alpha \cos \beta (\cos \phi \sin \theta \sin \psi - \sin \phi \cos \psi)] \quad (1.26) \end{aligned}$$

Now the equations are summarized in a state space form that will be used for control, disturbance estimation and compensation. The whole state equations are reorganized as follow:

$$\mathbf{x} = [u, v, w, p, q, r, \phi, \theta, \psi, x_N, y_E, h]^T \quad (1.27)$$

$$\dot{\mathbf{x}} = \mathbf{f}(\mathbf{x}) + \mathbf{g}(\mathbf{x})\mathbf{u} \quad (1.28)$$

The aircraft parameters are given in table 1.1.

$m = 1247[\text{kg}]$	$C_{L0} = 0.0242[-]$
$I_x = 1421[\text{kg} \cdot \text{m}^2]$	$C_{L\alpha} = 4.44[\text{rad}^{-1}]$
$I_y = 4068[\text{kg} \cdot \text{m}^2]$	$C_{Leq} = 3.8[\text{rad}^{-1}]$
$I_z = 4786[\text{kg} \cdot \text{m}^2]$	$C_{L\delta e} = 0.355[\text{rad}^{-1}]$
$S = 17.09[\text{m}^2]$	$C_{D0} = 0.0206[-]$
$b = 10.18[\text{m}]$	$C_{D\alpha} = 0.33[\text{rad}^{-1}]$
$c = 1.74[\text{m}]$	$C_{Y\beta} = -0.564[\text{rad}^{-1}]$
$T/W = 0.36[-]$	$C_{Y\delta r} = 0.157[\text{rad}^{-1}]$
$C_{l\beta} = -0.074[\text{rad}^{-1}]$	$C_{m0} = 0.0371[-]$
$C_{lp} = -0.41[\text{rad}^{-1}]$	$C_{m\alpha} = -0.683[\text{rad}^{-1}]$
$C_{lr} = 0.107[\text{rad}^{-1}]$	$C_{meq} = -14.32[\text{rad}^{-1}]$
$C_{l\delta a} = 0.1342[\text{rad}^{-1}]$	$C_{m\delta e} = -0.923[\text{rad}^{-1}]$
$C_{l\delta r} = 0.118[\text{rad}^{-1}]$	$C_{np} = -0.0575[\text{rad}^{-1}]$
$C_{n\beta} = 0.071[\text{rad}^{-1}]$	$C_{n\delta a} = -0.00346[\text{rad}^{-1}]$
$C_{nr} = -0.125[\text{rad}^{-1}]$	$C_{n\delta r} = -0.0717[\text{rad}^{-1}]$
$AR = 6.04[-]$	$e = .8[-]$

Table 1.1: Aircraft parameters

To take into account the saturation of controls and their dynamic, the data used to model the actuators based on [?] are provided in table 1.2:

Actuator	min	max	Transfer function pole
δ_e	-20°	$+5^\circ$	10 rad/sec
δ_r	-24°	$+24^\circ$	10 rad/sec
δ_a	-24°	$+24^\circ$	10 rad/sec
δ_{th}	0%	100%	10 rad/sec

Table 1.2: Actuators model

Chapter 2

Baseline Controller

The baseline controller is the one that is used to guarantee the nominal performances of the system when no anomaly or parameter variation is present. The control system employed is the pole-placement. Starting from the non-linear model, using optimization method we can find the input for any given trim condition. Around this trim condition, the system is linearized and the matrices for lateral and longitudinal dynamics are used to design the baseline controller by pole-placement.

2.1 Trim as optimization problem

The aircraft trim can be solved numerically by defining a cost function that should be as low as possible.

$$J = \dot{x}R\dot{x}^T \quad (2.1)$$

where R is a weighting matrix and $\dot{x} = f(x) + g(x)u$.

The steps are :

- 1 define the trim point $V = V_{trim}, \phi = 0, \beta = 0, \dot{h} = 0, \dot{p} = \dot{q} = \dot{r} = 0$
- 2 select which variable have to be tracked and which can be free
- 3 define the weight matrix
- 4 define the cost function
- 5 run the *fmincon* MATLAB function to determine the state x and input u that realizes the minimum of the cost function J

A script is present in appendix.

2.2 System linearization

To linearize the system, the trim point is used and the A and B matrices are numerically computed for both longitudinal and lateral dynamic. A script is attached in appendix. The matrices for the longitudinal dynamics at $V_{trim} = 50[m/s]$, $\rho = \rho_0$ are reported:

$$A_{LONG} = \begin{bmatrix} -0.0171 & 0.2696 & -5.0280 & -9.7592 \\ -0.1992 & -1.8903 & 48.3540 & -0.9974 \\ 0.0155 & -0.1519 & -2.7816 & 0 \\ 0 & 0 & 1.0000 & 0 \end{bmatrix} \quad (2.2)$$

$$B_{LONG} = \begin{bmatrix} 0.2990 & 3.2373 \\ -7.4577 & 0 \\ -10.3196 & 0 \\ 0 & 0 \end{bmatrix} \quad (2.3)$$

with $x_{LONG} = [u, w, q, \theta]$ and $u_{LONG} = [\delta_e, \delta_{th}]$.

The matrices for lateral dynamics at the same trim condition are:

$$A_{LAT} = \begin{bmatrix} -0.2367 & 5.0836 & -49.7409 & 9.7592 \\ -0.2776 & -7.8278 & 2.0429 & 0 \\ 0.0791 & -0.3259 & -0.7085 & 0 \\ 0 & 1 & 0.1022 & 0 \end{bmatrix} \quad (2.4)$$

$$B_{LAT} = \begin{bmatrix} 0 & 3.2945 \\ 25.1678 & 22.1297 \\ -0.1926 & -3.9921 \\ 0 & 0 \end{bmatrix} \quad (2.5)$$

with $x_{LAT} = [v, p, r, \phi]$ and $u_{LAT} = [\delta_a, \delta_r]$.

2.3 Pole Placement

The baseline controller is here presented: the eigenvalues have been placed by trial and error process in order to have the best trade-off in terms of control excursion and time response. For the longitudinal controller:

$$K_{LONG} = \begin{bmatrix} -0.0023 & 0.0211 & -0.3513 & -2.0495 \\ 0.7821 & -0.0455 & -0.2141 & 9.4073 \end{bmatrix} \quad (2.6)$$

and the system dynamic matrix A_m for the longitudinal dynamics becomes
 $A_{m_{LONG}} = A_{LONG} - B_{LONG} * K_{LONG}$

$$A_{m_{LONG}} = \begin{bmatrix} -2.5484 & 0.4105 & -4.2298 & -39.6007 \\ -0.2163 & -1.7333 & 45.7338 & -16.2823 \\ -0.0081 & 0.0654 & -6.4073 & -21.1505 \\ 0 & 0 & 1.0000 & 0 \end{bmatrix} \quad (2.7)$$

For the lateral controller:

$$K_{LAT} = \begin{bmatrix} -0.0103 & -0.3058 & 0.7571 & -0.0882 \\ -0.0075 & 0.1207 & -0.5185 & 0.0935 \end{bmatrix} \quad (2.8)$$

and the system dynamic matrix A_m for the lateral dynamics becomes $A_{m_{LAT}} = A_{LAT} - B_{LAT} * K_{LAT}$

$$A_{m_{LAT}} = \begin{bmatrix} -0.2487 & 3.5077 & -57.4013 & 9.3436 \\ 0.2762 & -2.1581 & -8.4645 & 0.2148 \\ 0.0491 & 0.2180 & -3.6208 & 0.5132 \\ 0 & 1.0000 & 0.0682 & 0.0000 \end{bmatrix} \quad (2.9)$$

Chapter 3

L1AC

In this chapter the *L1AC* is presented in its main components and mathematical definition. It is important to notice that the L1AC unlike other adaptive controllers such as MRAC, compensates only the uncertainties within the controller bandwidth by a low-pass filter $D(s)$.

The starting reference system is given by the following equation:

$$\dot{x} = Ax + B_m u + f \quad (3.1)$$

where f contains all the modeling uncertainties due to unmodeled dynamics, external disturbances and commands cross-coupling. The above system can be represented also in the following way:

$$\dot{x} = A_m x + B_m(\omega u_{ad} + \sigma_1) + B_{um}\sigma_2 \quad (3.2)$$

and the total control law is $u = -K_{baseline}x + u_{ad}$, with $A_m = A - B_m K_{baseline}$. Where B_m is the control channel matrix, σ_1 also known as matched disturbance, σ_2 knowns as unmatched disturbance, and ω is the matrix that represents the cross-coupling among different control input.

3.1 State Predictor

The state predictor equation is here reported:

$$\dot{\hat{x}} = A_m \hat{x} + B_m(\omega_0 u_{ad} + \hat{\sigma}_1) + B_{um}\hat{\sigma}_2 \quad (3.3)$$

with $\omega_0 = I_m$.

3.2 Adaptation Law

The adaptation laws are used to estimate the matched and unmatched uncertainties. Herein the computational steps are reported:

$$\tilde{x} = \hat{x} - x \quad (3.4a)$$

$$\mu(T_s) = e^{A_m T_s} \tilde{x} \quad (3.4b)$$

$$\phi(T_s) = A_m^{-1} (e^{A_m T_s} - I_n) \quad (3.4c)$$

$$\begin{bmatrix} \hat{\sigma}_1 \\ \hat{\sigma}_2 \end{bmatrix} = - \begin{bmatrix} I_m & \cdots \\ \cdots & I_{n-m} \end{bmatrix} [B_m \ B_{um}]^{-1} \phi(T_s)^{-1} \mu(T_s) \quad (3.4d)$$

3.3 Control Laws

As stated previously, $u(t) = -K_{baseline} x + u_{ad}$.

Where K is such that $A_m = A - BK_{baseline}$ is Hurwitz.

The adaptive control law is the following:

$$u_{ad} = -K_{ad} D(s) \hat{\eta} \quad (3.5a)$$

$$\eta = \omega_0 u_{ad} + \hat{\eta}_1 + \hat{\eta}_2 - r_g \quad (3.5b)$$

$$\hat{\eta}_1 = \hat{\sigma}_1 \quad (3.5c)$$

$$\hat{\eta}_{2m}(s) = H_m^{-1}(s) H_{um}(s) \hat{\sigma}_2(s) \quad (3.5d)$$

$$r_g(s) = K_g(s) r(s) \quad (3.5e)$$

The tuning parameters are $D(s)$ and K_{ad} that have to be choosen such that:

$$C(s) = \omega_u K_{ad} D(s) (I_m + \omega_u K_{ad} D(s))^{-1} \quad (3.6)$$

for all possible ω_u is stable and has DC gain $C(0) = I_m$; furthermore $C(s)H_m^{-1}$ has to be a strictly proper transfer function. The matrices H_{um} and H_m are herein defined:

$$H_m(s) = C(sI_n - A_m)^{-1} B_m \quad (3.7a)$$

$$H_{um}(s) = C(sI_n - A_m)^{-1} B_{um} \quad (3.7b)$$

The feedforward prefilter K_g is chosen such that it decouples the signals, such that $M(s) = C(sI_n - A_m)^{-1} B_m K_g$ has off-diagonal elements zero DC gain and diagonal gain one:

$$K_g = -(CA_m^{-1}B_m)^{-1} \quad (3.8)$$

Chapter 4

Application to fixed-wing aircraft

To test the robustness of the *L1AC* the aircraft parameters in 1.1 have been strongly modified. The results are hereafter presented as well as the navigation control law for the slowest variable (altitude and heading).

4.1 Navigation Control Law

For the control of altitude h and heading ψ simple PID are used respectively to compute θ_{ref} and ϕ_{ref} , since the uncertainties are not related to kinematic equations of motion, but rather to the faster inner dynamics variables.

PID gains have been tuned by using the tune function in the *Simulink Control Design Toolbox*. A scheme of the overall flight control system is herein reported in 4.1.

4.2 Longitudinal Controller

The L1AC for the longitudinal side, is realized with the following matrices:

$$A = A_{LONG} \quad (4.1a)$$

$$B_m = B_{LONG} \quad (4.1b)$$

$$B_{um} \text{ s.t. } B_m^T B_{um} = 0 \quad (4.1c)$$

$$C = \begin{bmatrix} 1 & 0 & 0 & 0 \\ 0 & 0 & 0 & 1 \end{bmatrix} \quad (4.1d)$$

$$K_{baseline} = K_{LONG} \quad (4.1e)$$

$$A_m = A - B_m K_{baseline} \quad (4.1f)$$

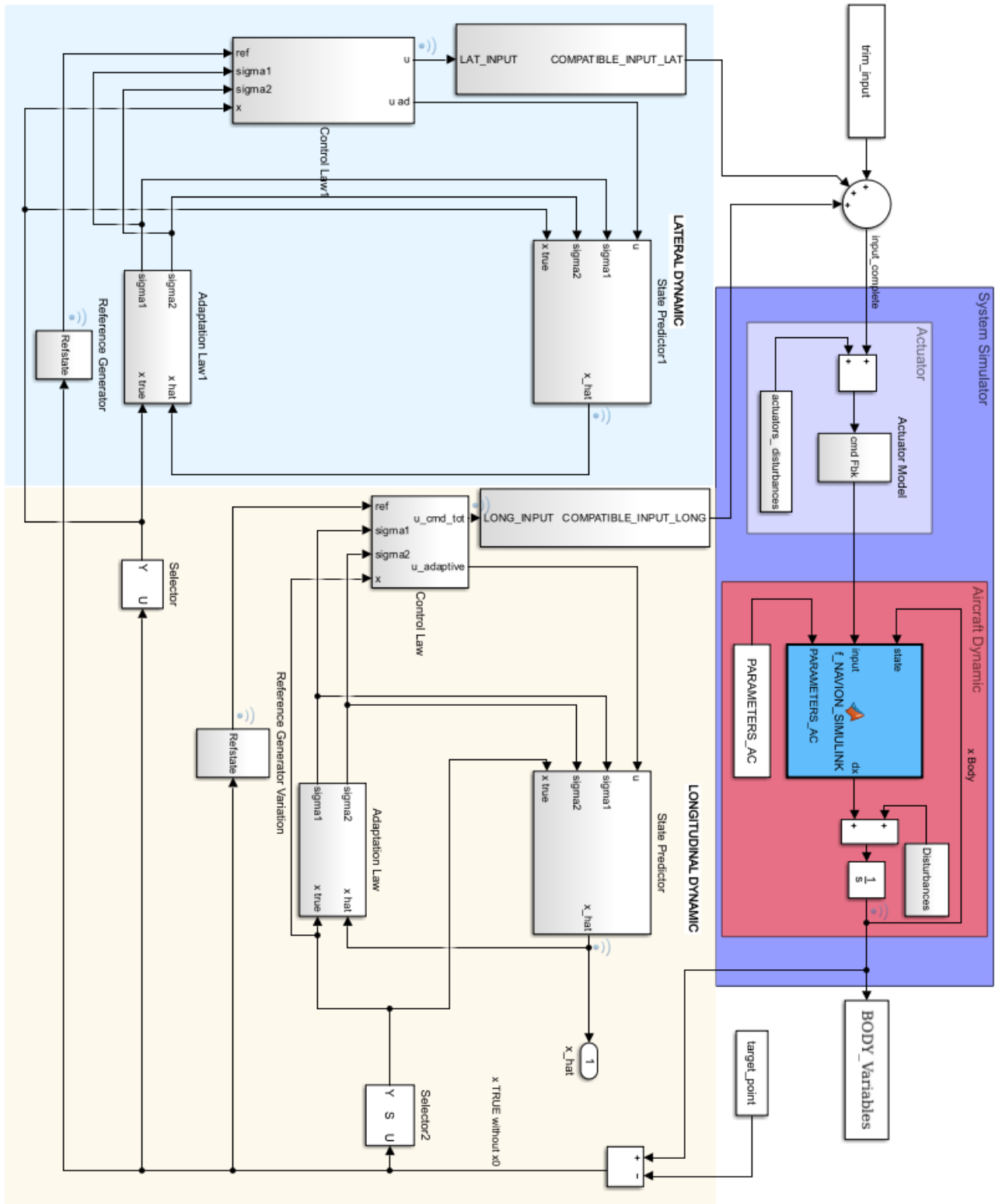


Figure 4.1: Overall Scheme

The variables to be tracked are u_{REF} and $\theta_{REF} = PID(h_{REF} - h)$. The filter $D(s)$ and K are selected to be:

$$D(s) = \frac{1}{s+1} \quad (4.2a)$$

$$K_{ad} = 20 I_2 \quad (4.2b)$$

$$T_s = 0.01 \quad (4.2c)$$

4.3 Lateral Controller

The L1AC for the lateral dynamics, is realized with the following matrices:

$$A = A_{LAT} \quad (4.3a)$$

$$B_m = B_{LAT} \quad (4.3b)$$

$$B_{um} \text{ s.t. } B_m^T B_{um} = 0 \quad (4.3c)$$

$$C = \begin{bmatrix} 1 & 0 & 0 & 0 \\ 0 & 0 & 0 & 1 \end{bmatrix} \quad (4.3d)$$

$$K_{baseline} = K_{LAT} \quad (4.3e)$$

$$A_m = A - B_m K_{baseline} \quad (4.3f)$$

The variables to be tracked are $v_{REF} = 0$ and $\phi_{ref} = PID(\psi_{ref} - \psi)$. The filter $D(s)$ and K are selected to be:

$$D(s) = \frac{1}{0.1s + 1} \quad (4.4a)$$

$$K_{ad} = 40 I_2 \quad (4.4b)$$

$$T_s = 0.01 \quad (4.4c)$$

4.4 Simulation results

The simulation results are herein reported. In the first case, none uncertainty is introduced in the parameters. The nominal behavior is used as benchmark for the performance robustness of the adaptive controller.

The initial conditions are $TAS = 60 \text{ m/s}$ and $h = 10 \text{ m}$ and $\psi = 0^\circ$.

The reference TAS is increased by 10 m/sec , while the altitude reference is 0 meters and the $\psi = 10^\circ$

4.4.1 None Uncertainties in the parameters: Nominal Condition

The result of the L1AC with nominal parameters is compared in the following sections. The performance are satisfactory as expected.

4.4.2 Uncertainties in the parameters

Herein are reported the results of parameters uncertainties, starting from the same initial condition as the none uncertainties case. As can be noted the *L1AC* is able to compensate for the uncertainties retaining the same performances.

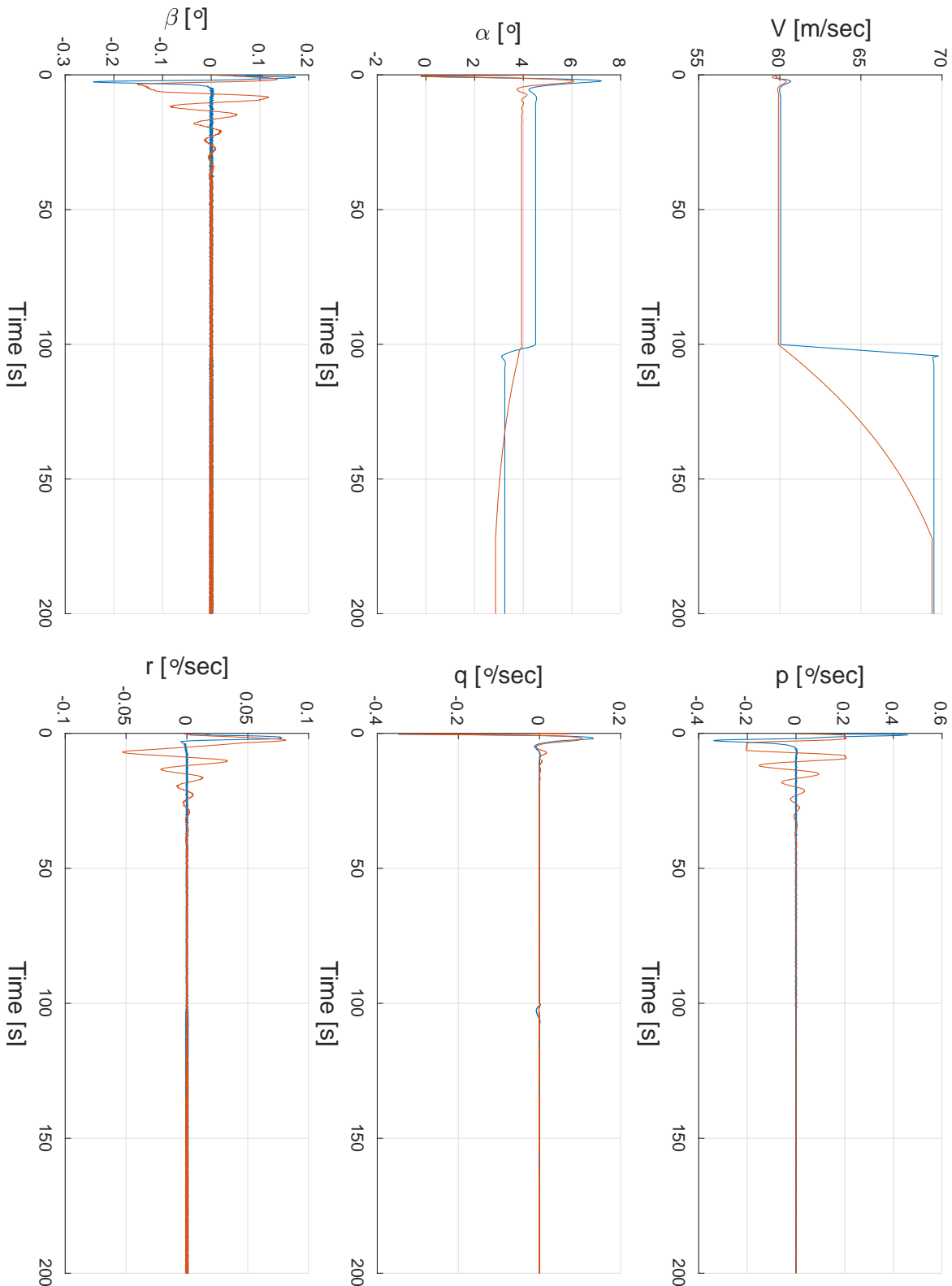


Figure 4.2: State Variable Comparison 1.a

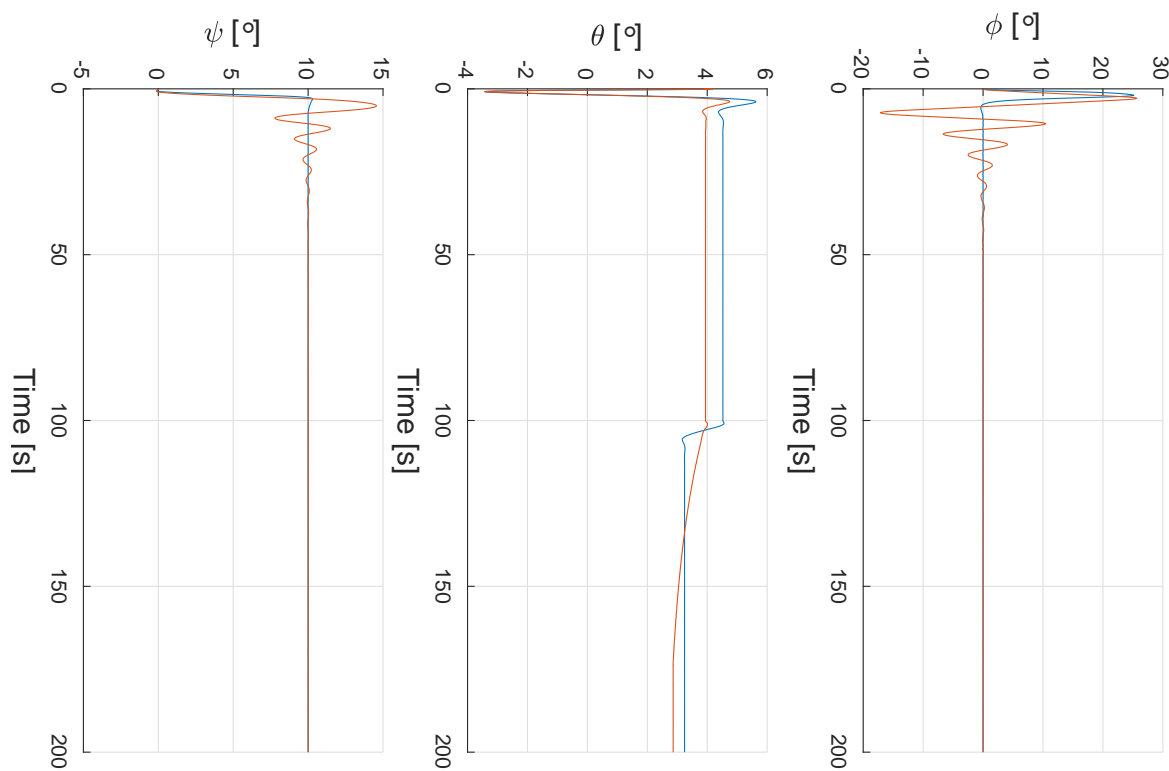


Figure 4.3: State Variable Comparison 1.a

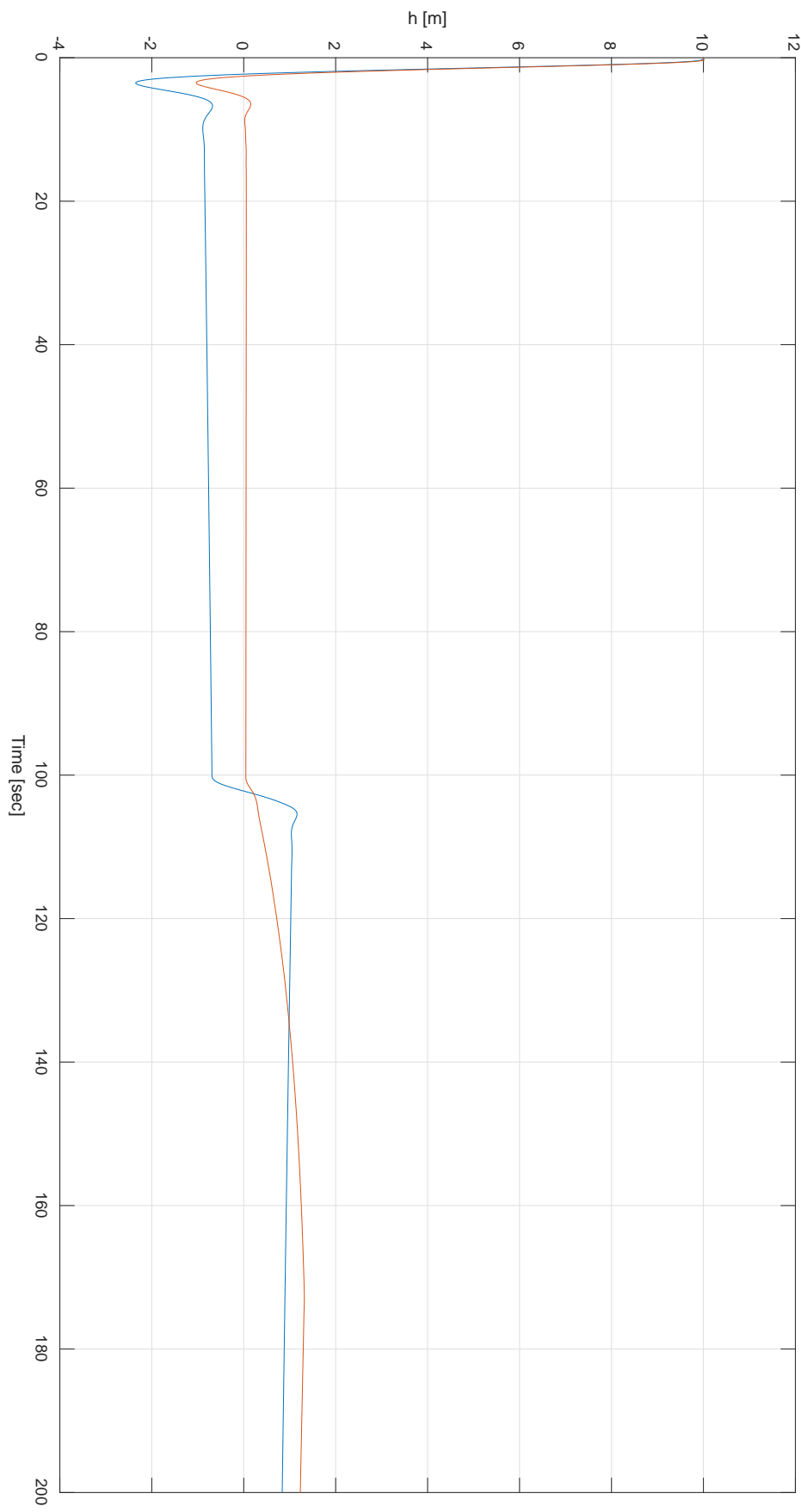


Figure 4.4: Altitude performance

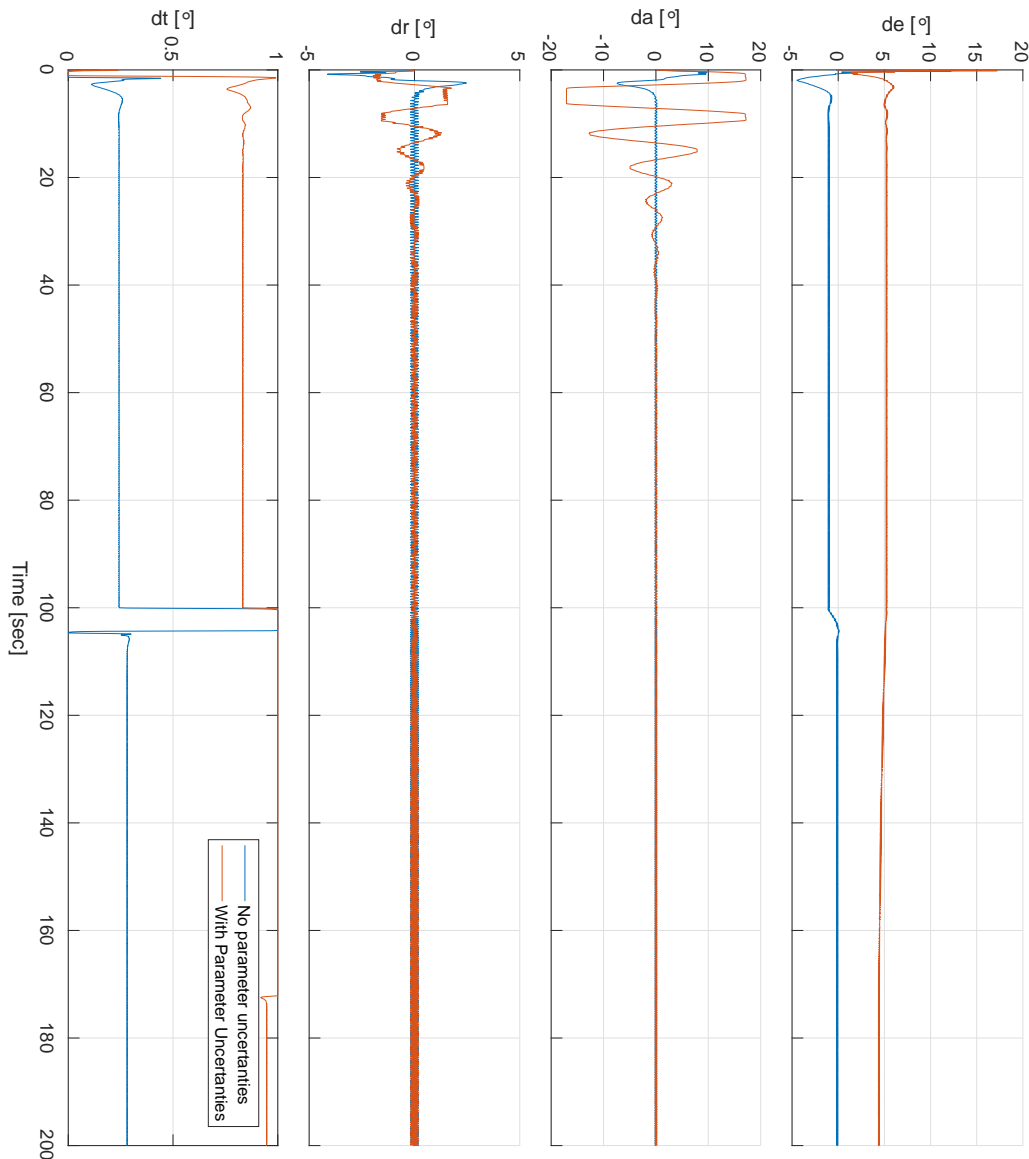


Figure 4.5: Input history

4.4.3 Uncertainties in the parameters and input oscillations

In this case we add oscillation to the input channels. Depending on the disturbance frequency, the *L1AC* is able to compensate completely or partially within the control channel bandwidth. As can be noted the performances are quite satisfactory given the amount of disturbances the FCS has to compen-

sate when compared to the only baseline controller (it crush the simulation). A comparison is given between only input + disturbances and the case where parameters uncertainties is added on top of them.

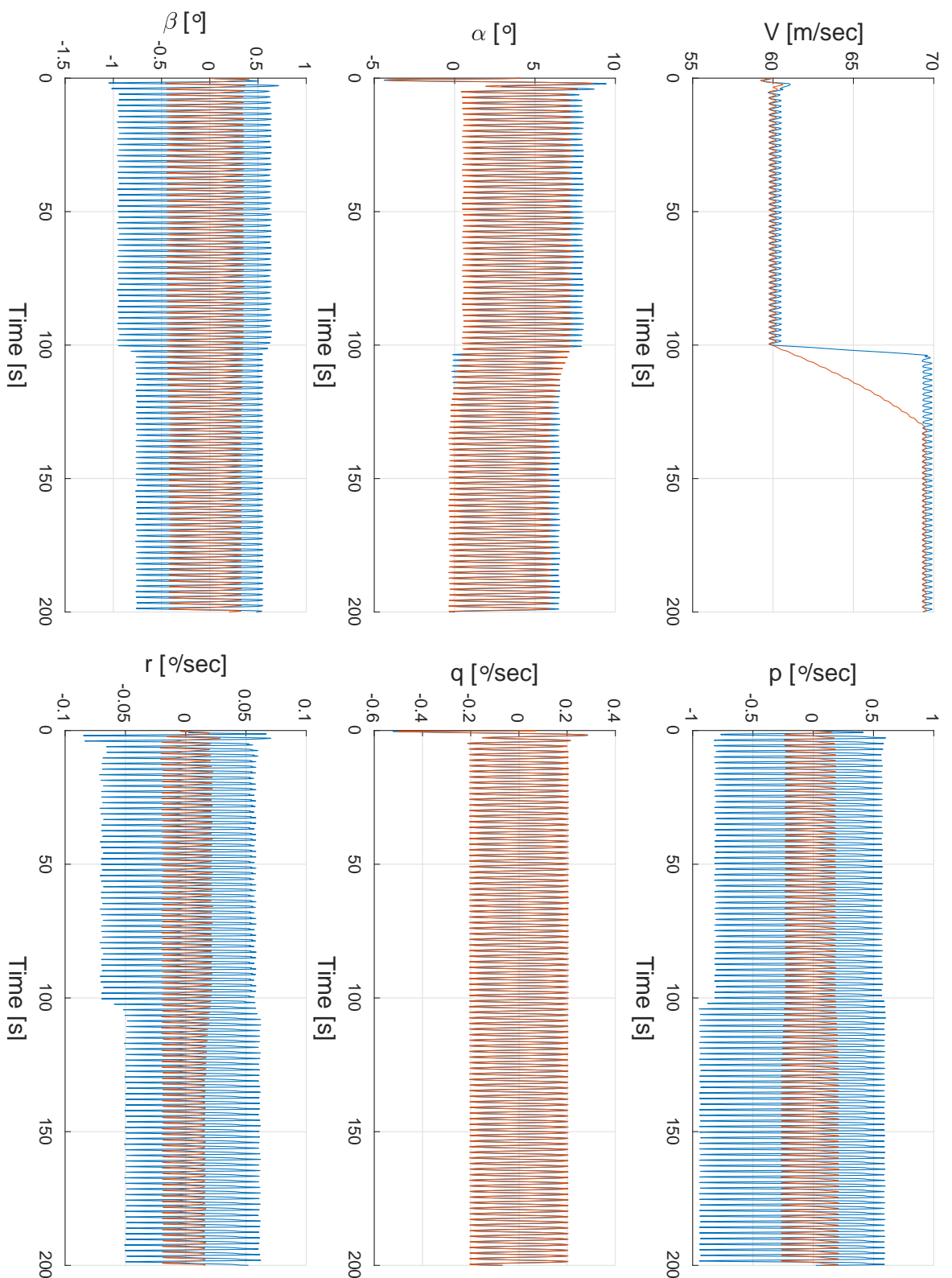


Figure 4.6: State Variable Comparison 1.a

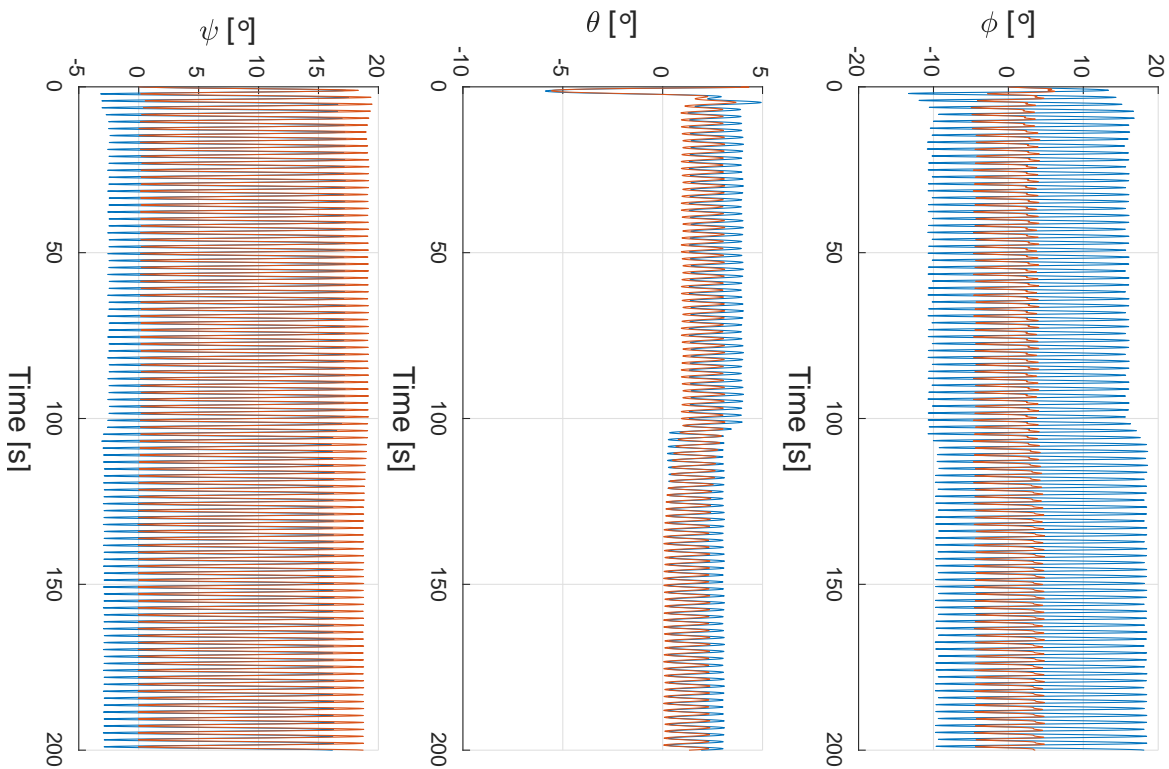


Figure 4.7: State Variable Comparison 2.a

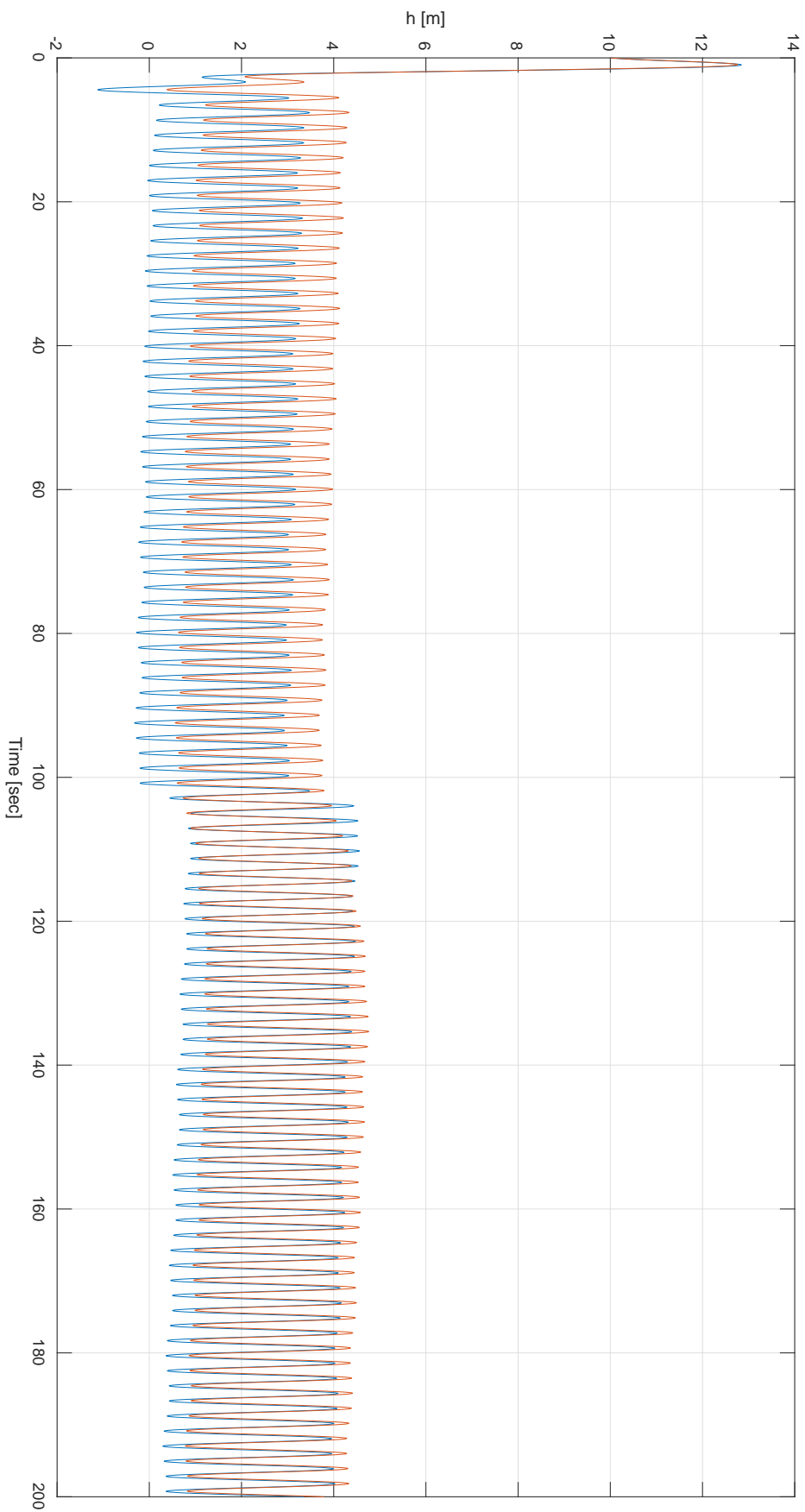


Figure 4.8: Altitude performance

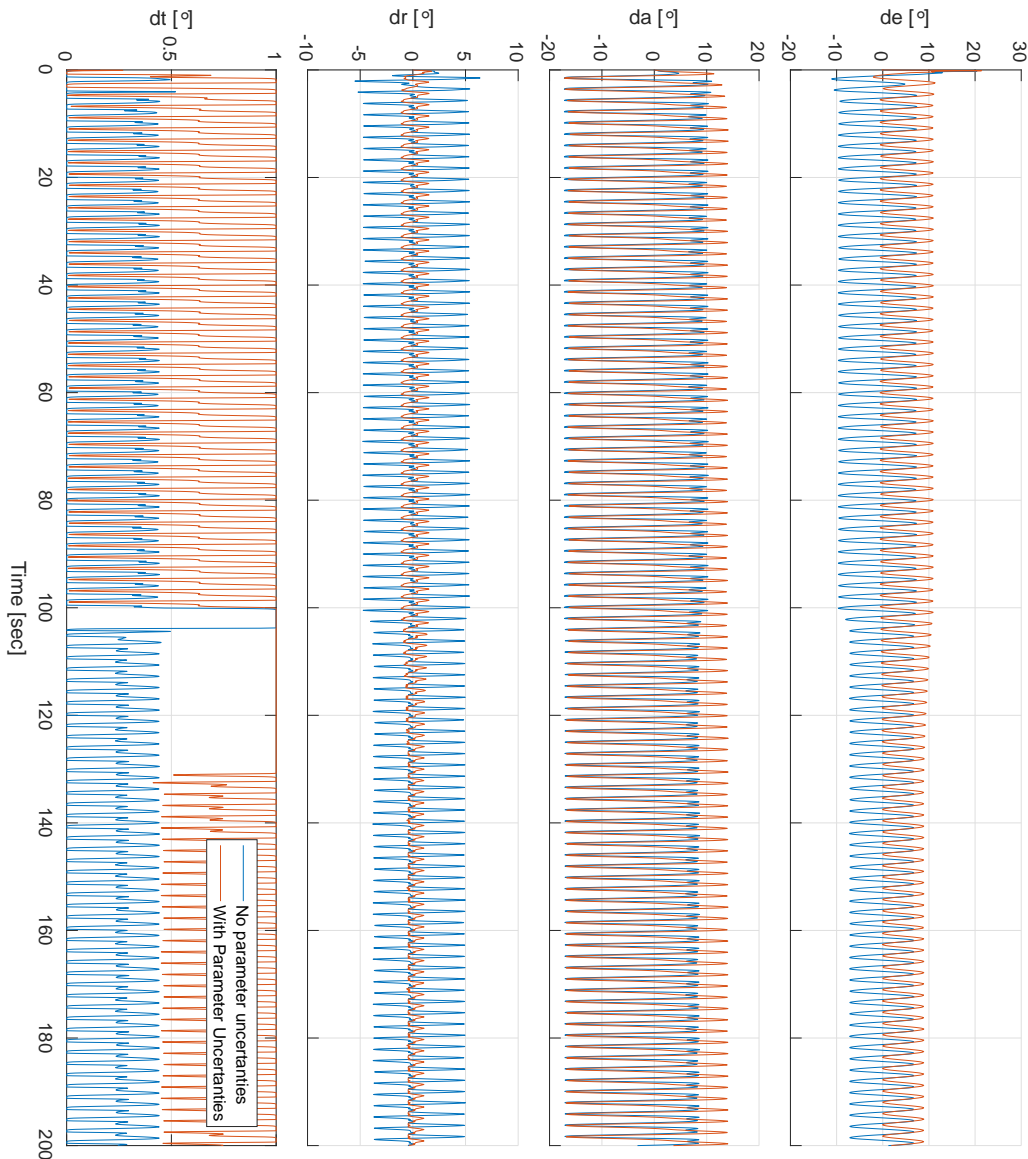


Figure 4.9: Input history

4.5 Dealing with time delay and sampling

To reproduce the fact that control laws are executed on microprocessors, lag effects are taken into account by zero-order hold. Zero-order-hold have been used to simulate the constant input between two time steps computation at $100Hz$, $T_s = 1/100 sec$. Simulations have been performed taking into account time-delay, uncertainties in the parameters and input oscillations

contemporary and can be seen that time delay is crucial to stability but L1AC can cope with it well. Results are reported where the controller frequency changes: frequency is changed into 25 Hz instead of 100Hz. Results are not extremely good in absolute, but thinking at the fact that is a very different situation, are relatively good. The way to improve the robustness in case of reduction of frequency of the FCS is to relax the requirements in terms of pole placement: the behavior should be slower to do not have high oscillation; this agrees with the fact that a controller should be as fast as the dynamic we want to give to the closed loop system.

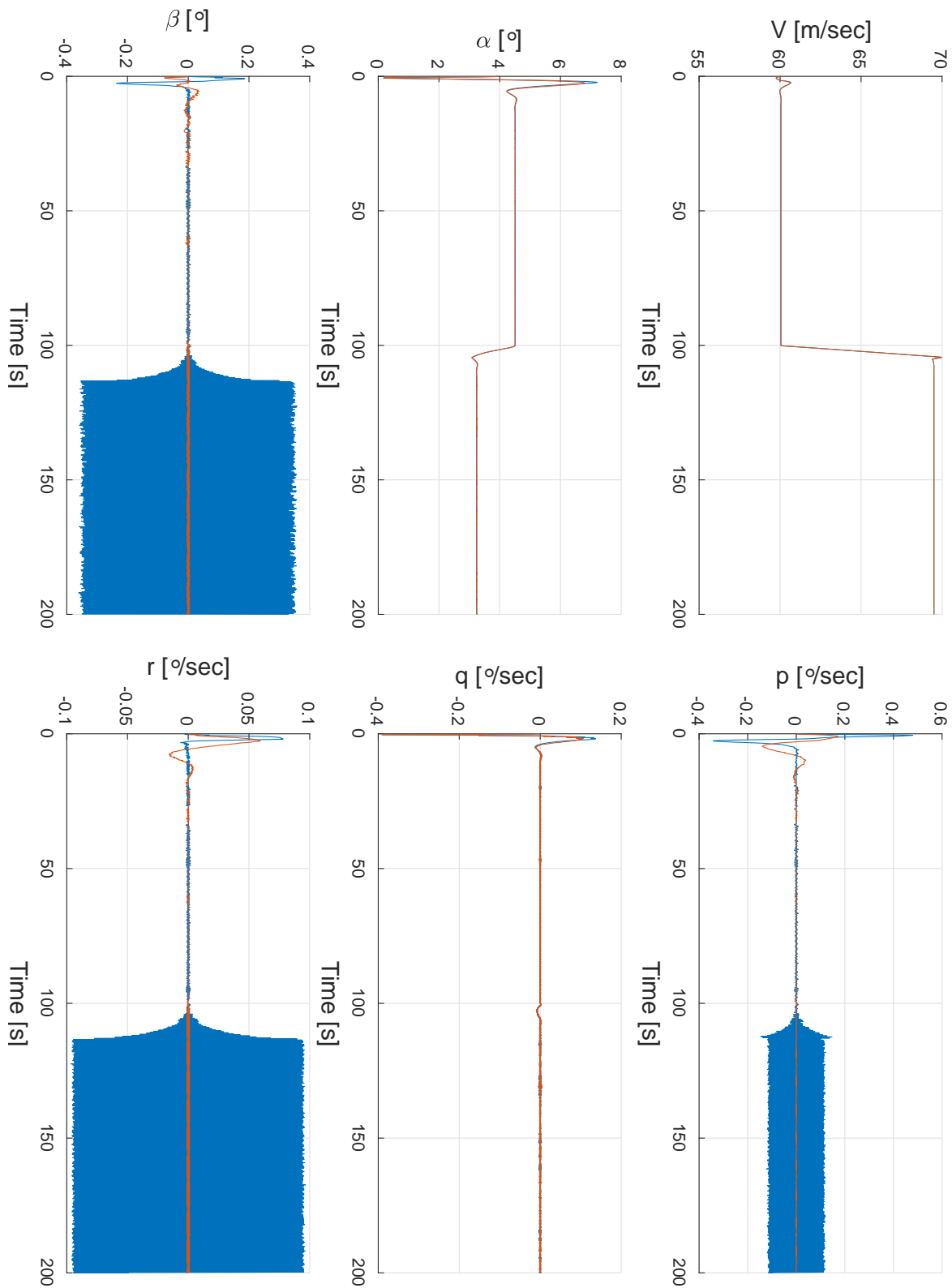


Figure 4.10: State Variable Comparison 1.a

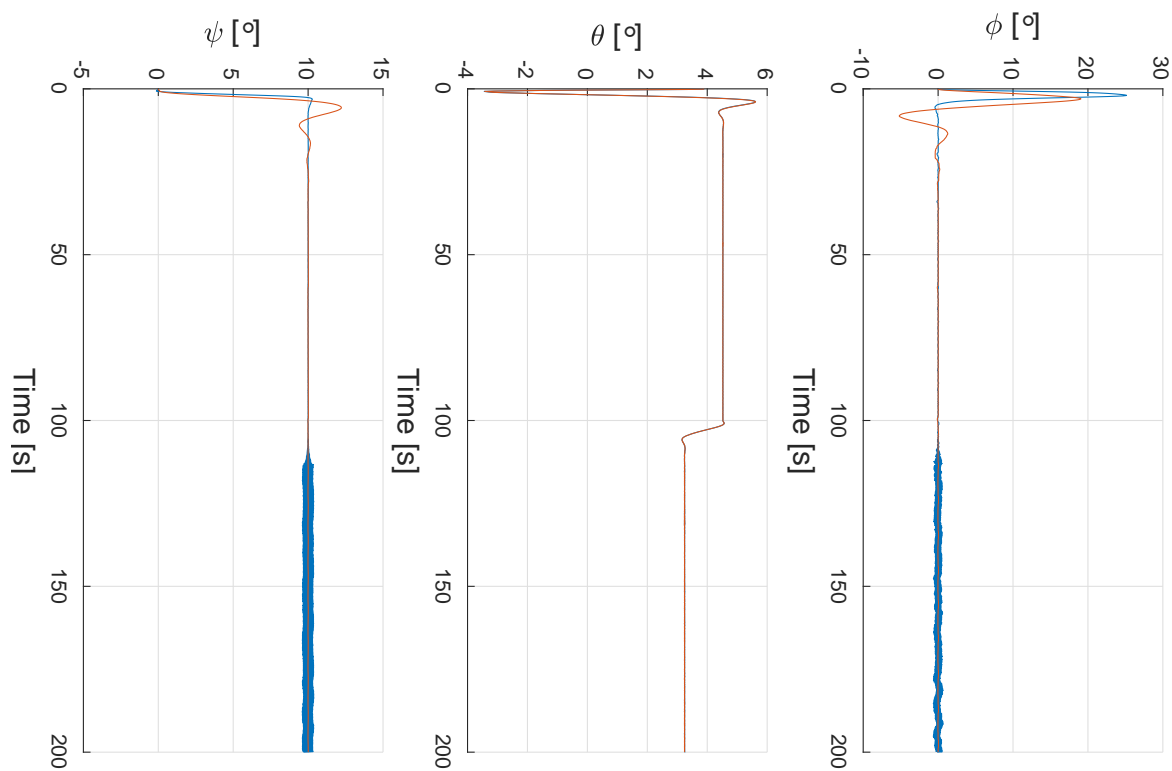


Figure 4.11: State Variable Comparison 2.a

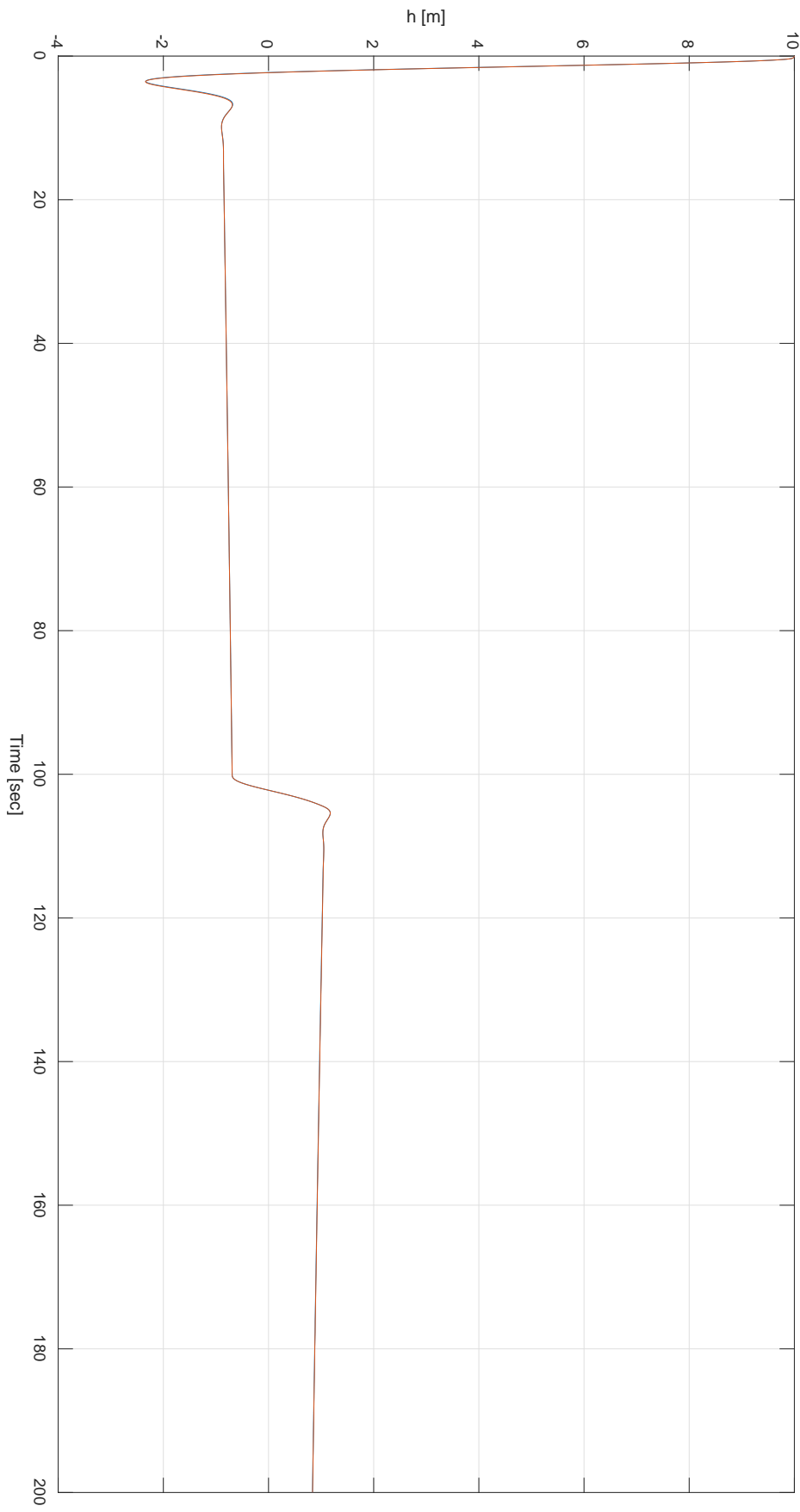


Figure 4.12: Altitude performance

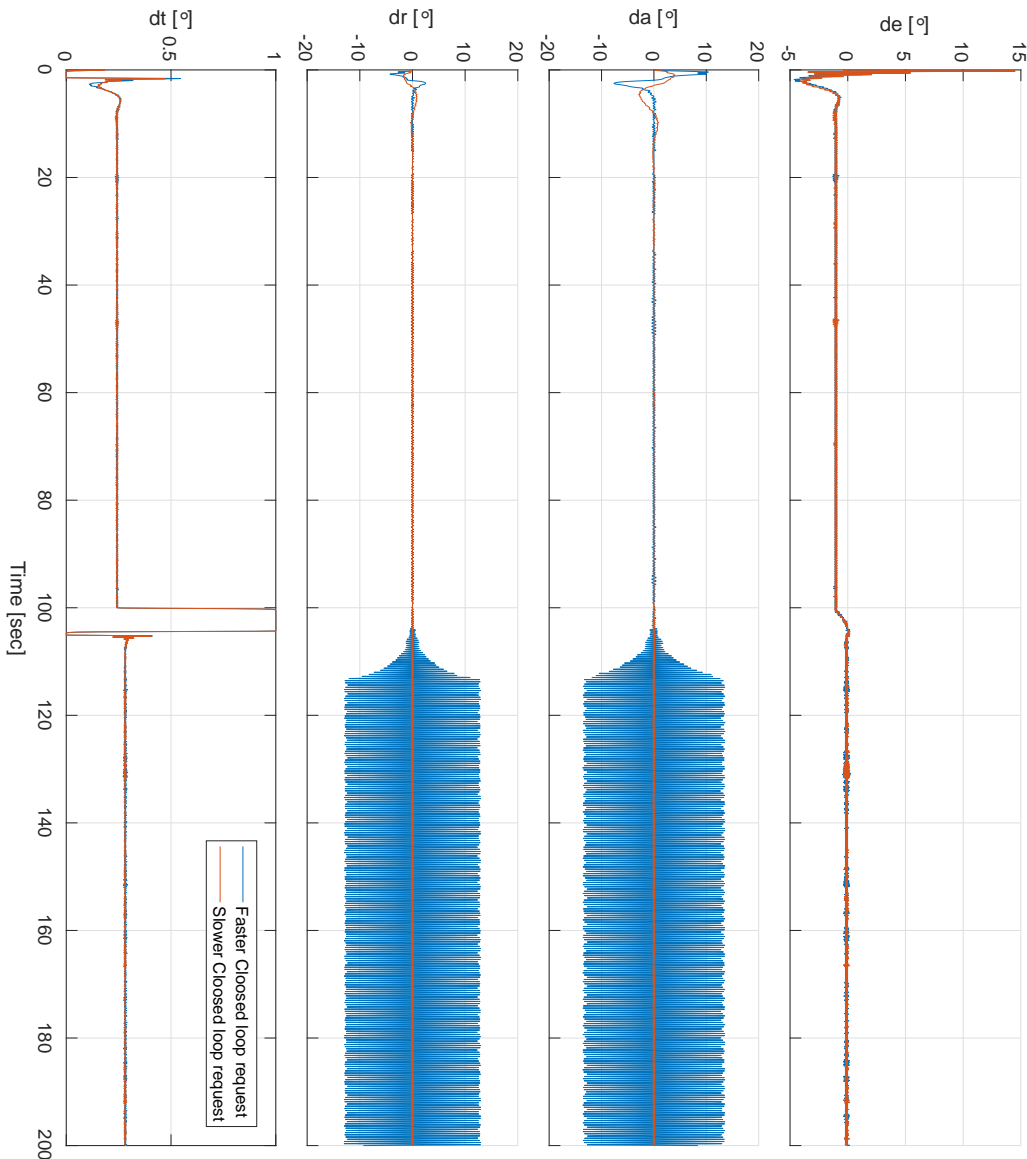


Figure 4.13: Input history

4.6 MONTECARLO ANALYSIS

Is engineering practice nowadays, to perform Montecarlo simulations in order to have more confidence about the robustness of the FCS.

In the following, the main figures describing the aircraft behavior with different sets of parameters are provided. The results are promising, and agree with other published papers.

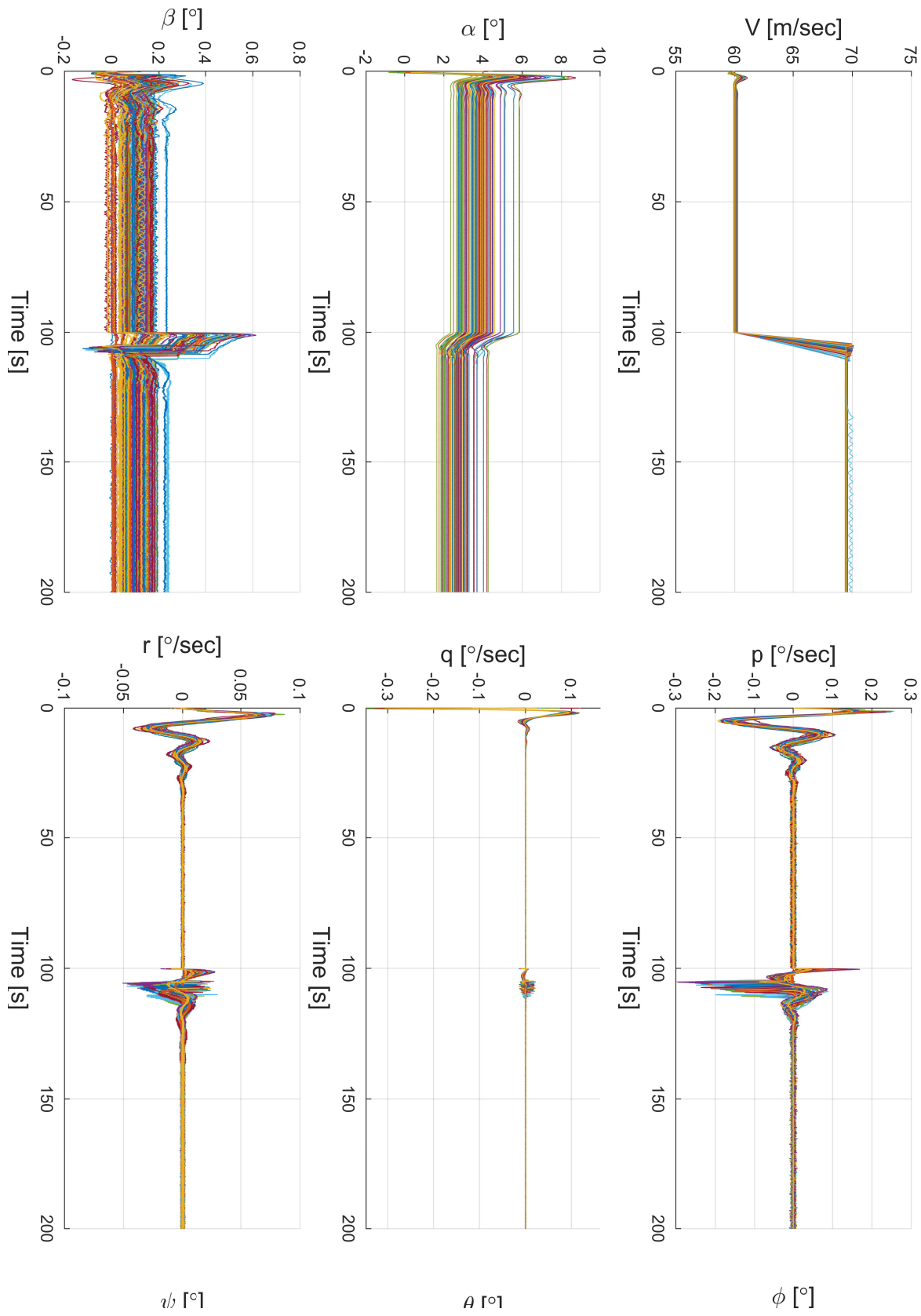


Figure 4.14: State Variable Comparison 1.a

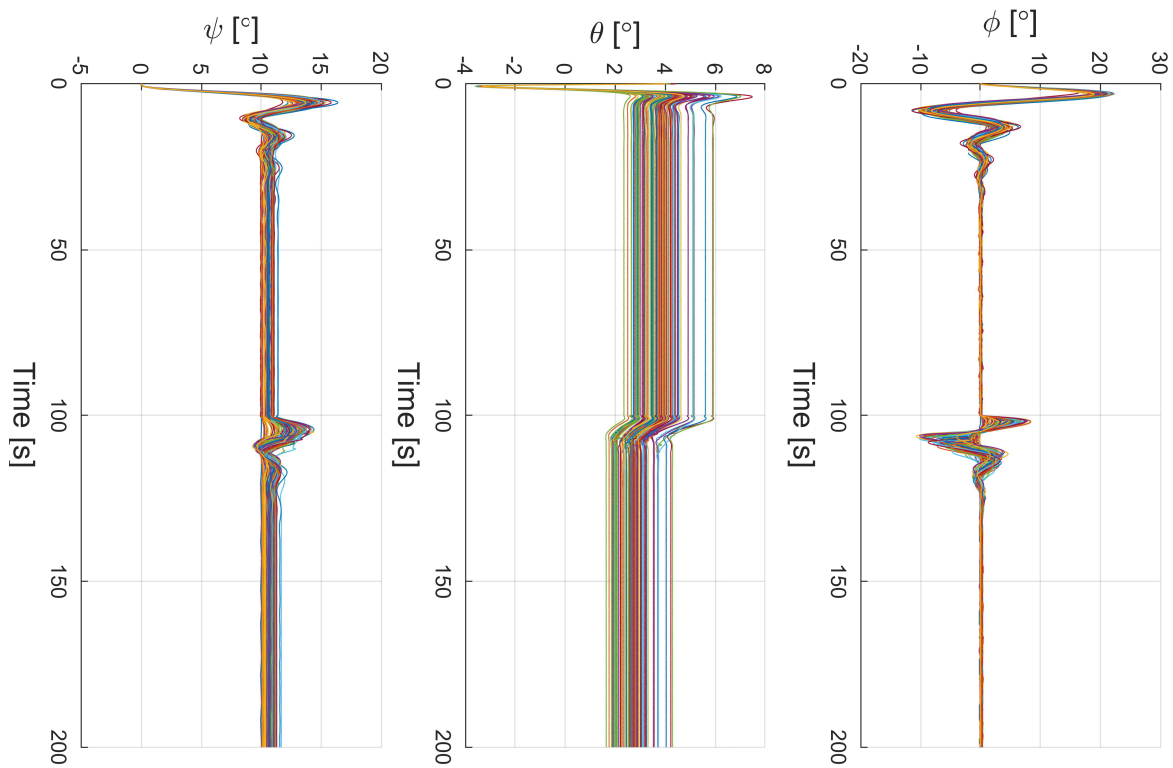


Figure 4.15: State Variable Comparison 2.a

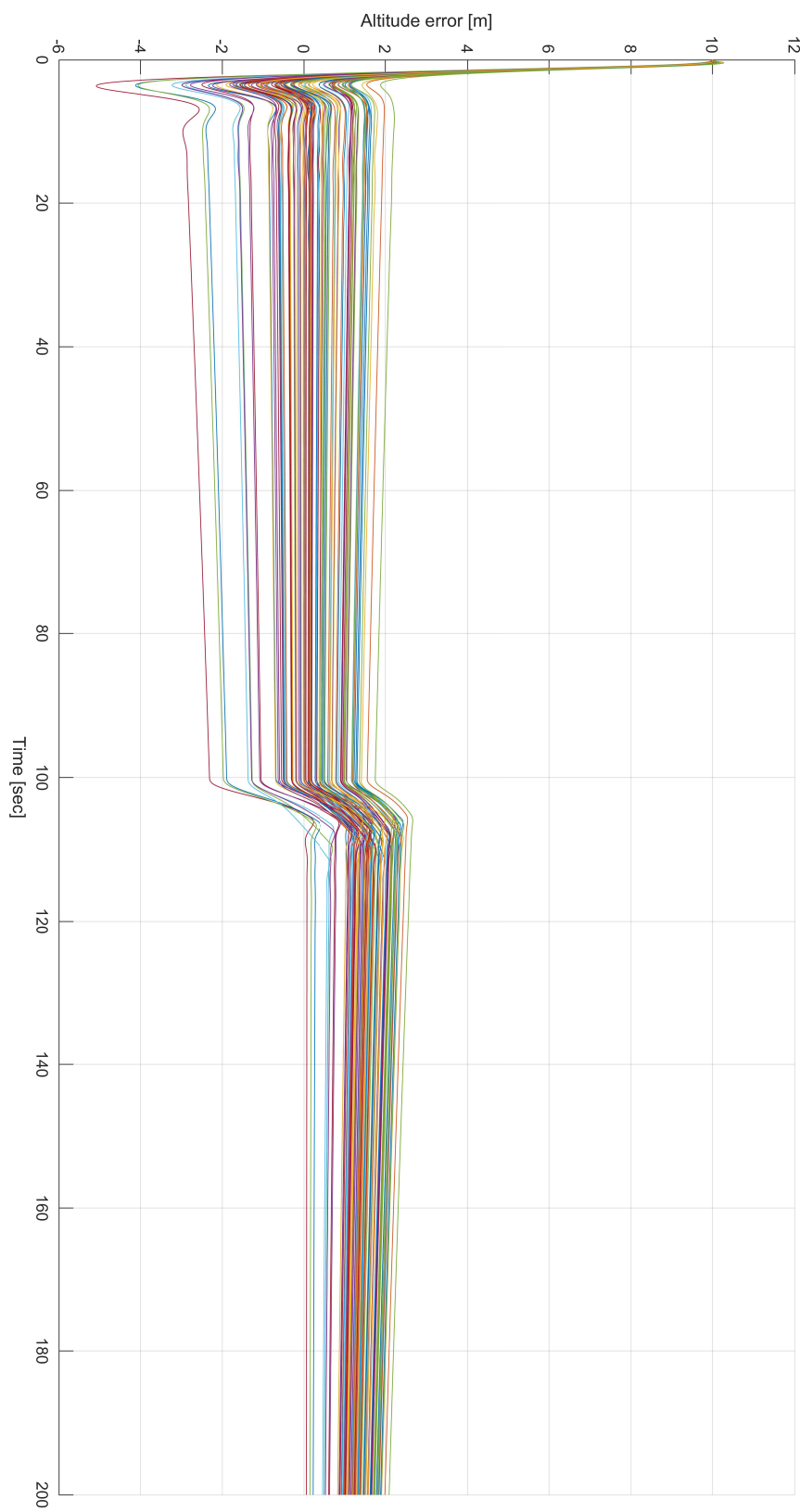


Figure 4.16: Altitude performance

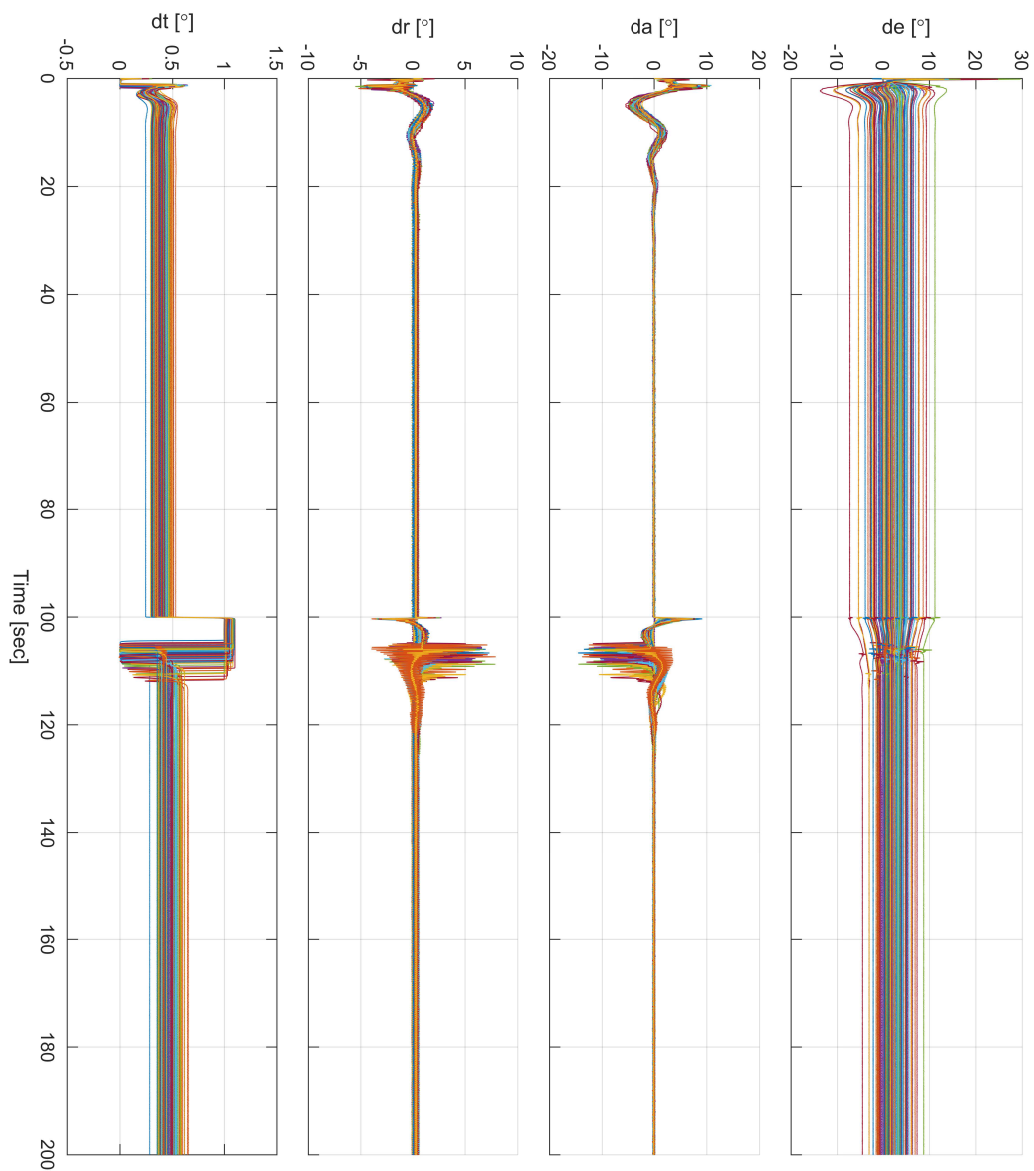


Figure 4.17: Input history

Conclusion

L1AC has demonstrated to be robust with respect to both actuator disturbances, parameter variation and external disturbances.

L1AC thanks to its nature of being an adaptive control scheme, is able to retain stability even if aircraft parameters change compared to those used to design the *Baseline controller*. This is a very interesting feature since it can eliminate, or reduce, the need of gain scheduling.

Simulations have been performed for different aircraft's parameters, successfully. This means that the FCS is able to regain its performances automatically and ensure a safe flight.

In this sense a very interesting application would be the implementation on a micro-controller and real flight testing on two different aircrafts; a control system of this kind seems to be quite universal in the sense that seems to do not require gain scheduling or retuning, but only flight tests will tell us if *L1AC* is a feasible solution for a ready-to-fly control system no matter the aircraft dynamic/stability.